Organic & Biomolecular Chemistry

Accepted Manuscript

ROYAL SOCIETY OF CHEMISTRY

www.rsc.org/obc

Journal Name

ARTICLE

A Pyrene-bridged Macrocage Showing No Excimer Fluorescence†

Hirokuni Shionari,[a] Yusuke Inagaki,[a] Kentaro Yamaguchi,[b] and Wataru Setaka*[,a]

Received 00th January 20xx,
Accepted 00th January 20xx

DOI: 10.1039/x0xx00000x

www.rsc.org/

Pyrene is a common organic luminescent material. To improve the fluorescence properties of pyrene, we have designed a pyrene-2,7-diyl bridged macrocage in which the pyrene moiety is sterically protected by the outside alkyl chains. The macrocage shows intense fluorescence from a monomeric excited state without excimer fluorescence even in saturated solution, although parent pyrene shows excimer fluorescence in highly concentrated solutions. These results indicates that the steric shielding by the cage prevents the formation of the excimer. Intensities of florescence in the presence of nitrobenzene were investigated to clarify cage effects on fluorescence quenching. Lower efficiency of the fluorescence quenching caused by intermolecular collision between the caged pyrene (fluorophore) and nitrobenzene (quencher) was revealed by analysis of the bimolecular quenching constants k_q.

Introduction

Pyrene has been used as a fluorescent probe in multi-molecular systems because of its high fluorescence quantum yield.[1] For instance, pyrene derivatives have frequently been used as efficient fluorescent moieties in molecular imaging in biological systems and fluorescent chemosensors.[1] However, under high concentration conditions, the fluorescence spectra of pyrene derivatives show a broad blue emission from the excimer as well as a violet emission from the unassociated (monomer) molecule. The appearance of excimer fluorescence can sometimes disturb quantitative analysis when using a pyrene fluorescent agent. In order to improve the fluorescence properties of fluorescent molecules that are likely to form excimers, we propose a caged fluorescent probe. In this study, a cage-like cyclophane of pyrene (**1**) was first designed and synthesized (Chart 1). The basic fluorescence properties of the cage were then investigated and compared with those of the non-caged isomer **1i**.

Macrocage molecules with a bridged π-electron system, such as **1**, were recently investigated as molecular gyroscopes and gyrotops because the macrocage framework protects the rotation of an interior π-rotor by Garcia-Garibay's group,[2] Gladysz's group,[3] and our group.[4,5] We have previously reported phenylene, thiophene-2,5-diyl, and naphthalene-1,4-diyl bridged macrocages, and the dynamics of the π-rotor in disilaalkane macrocages have also been reported.[4] As studies of the chemistry of such cage-like cyclophanes have only been reported by a few research groups,[2-5] the properties and functions of the cage in these molecules have been investigated very recently.[6]

Chart 1

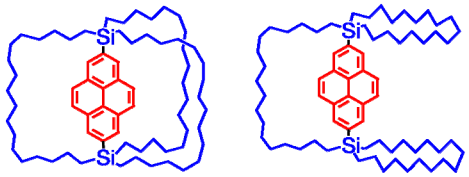

1 **1i**

Many caged compounds exhibit host–guest chemistry. Yorozu, Hoshino, and Imamura reported the fluorescence of a pyrene inclusion complex with cyclodextrins; a pyrene dimer was formed in the γ-cyclodextrin cavity.[7a] Other studies on the inclusion of pyrene guest inside a host have been reported by Fujita,[7b] Stoddart,[7c] and Gibb[7d]. These supramolecular complexes have many advantages such as easy synthesis and excellent properties.

The aim of this study is a development of a cage with novel steric functionality to improve the photophysical properties of the fluorophore without the supramolecular approach. The cage effects of small molecules such as **1** can be easily investigated theoretically; this may be an advantage of small molecules over supramolecular complexes. The basic studies of the properties of this simple cage will implement novel principles of the molecular design for new functional molecules. For this reason, a novel cage-like cyclophane with a fluorophore was synthesized, and its basic characteristics as a functional molecule were investigated.

[a] Division of Applied Chemistry, Faculty of Urban Environmental Sciences, Tokyo Metropolitan University, 1-1 Minami-Osawa, Hachioji, Tokyo 192-0397, Japan. E-mail: wsetaka@tmu.ac.jp.
[b] Faculty of Pharmaceutical Sciences at Kagawa Campus, Tokushima Bunri University, 1314-1 Shido, Sanuki, Kagawa 769-2193, Japan.

†Electronic Supplementary Information (ESI) available: [Details for spectroscopic data for the new compounds, details for X-ray crystallographic studies, details of fluorescence studies.]. See DOI: 10.1039/x0xx00000x

Results and Discussion

Design, synthesis, and Characterization

The pyrene-bridged macrocage was synthesized according to Scheme 1. The method was similar to that for phenylene-bridged derivatives.[4a,4f] As described in a previous report,[4a] a cage containing tetradecyl (C14) chains was found to be suitable for the phenylene-bridge, hence, a cage comprising octadecyl (C18) chains was thought to be suitable for the long pyrene-2,7-diyl bridge. Lithiation of 2,7-dibromopyrene followed by a substitution reaction with tri(9-decenyl)-chlorosilane[4a] in a hexane/tetrahydrofuran (THF) mixture in the presence of tetramethyldiaminoethane (TMEDA) afforded 2,7-bissilylpyrene **2** in 20% yield. The addition of TMEDA was necessary for the reaction to proceed because TMEDA activates dilithiopyrene. Indeed, the yield of compound **2** was only 5.5%, when the reaction was performed without TMEDA. The ring-closing metathesis (RCM) reaction of **2** by Grubbs' 1st generation catalysts followed by hydrogenation at the ethylene junctions gave a mixture of caged **1** and the non-caged isomer **1i**. Pure compounds of **1** and **1i** were isolated after treatment of the mixture by gel permeation chromatography (GPC) and the yields of **1** and **1i** from **2** were 5% and 51%, respectively. 2,7-Bis(trimethylsilyl)pyrene (**3**) was also newly synthesized as a reference compound in 56% yield by a substitution reaction of the corresponding dilithiopyrene with trimethylchlorosilane without TMEDA.

Single crystals of **1** were obtained by recrystallization from THF/MeOH (4:1 v/v) solution. Fig. 1a shows the molecular structure of the cage **1** determined by X-ray crystallography. The pyrene moiety of **1** was effectively surrounded by the cage. All of the carbons of the pyrene and the two silicon atoms lay in the same plane (RMS deviation from the least-squares plane is 0.0016 Å), and the bond lengths and angles of the bissilylpyrene moiety were in the normal range. Therefore, there is no strain inside the cage. The packing structure of **1** showed all of the molecules were arranged by their rotation axes, indicating that there are no intermolecular π-π interactions inside the cage compared with the crystal structure of **3** (Fig. 1b), because of the steric protection of the cage. Unfortunately, the non-caged isomer **1i** was obtained as a colorless oil at ambient temperature. Thus, the structure of the isomer was not identified by X-ray crystallography. In the structure of **3**, as determined by X-ray crystallography (Fig. 1b), the bond lengths and angles of the bissilylpyrene moiety of **3** are similar to those of **1**. However, the packing structure of **3** is totally different from that of **1**, indicating that intermolecular π-π stacking exists in the herringbone-like structure.

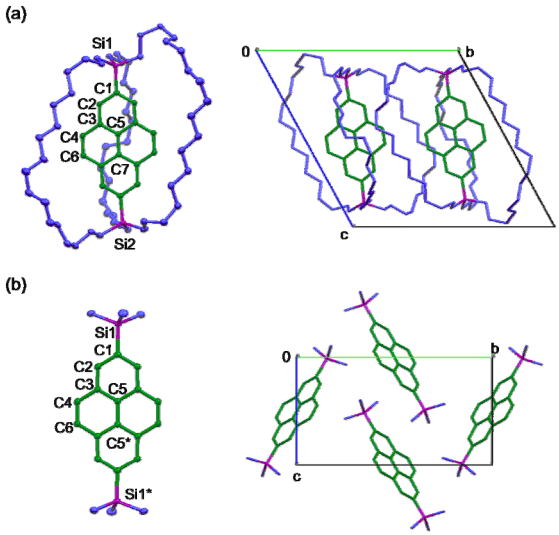

Fig. 1. Molecular structure of silylpyrenes as determined by X-ray crystallography (100 K) [left; molecular structure (30% thermal ellipsoid. Hydrogen atoms are omitted for clarity), right; packing structure]. (a) **1**; Selected bond lengths (Å) and bond angles (deg): Si1-C1 1.8882(16); C2-C3 1.400(2); C3-C4 1.423(2); Si1-C1-C2 121.18(12) C1-C2-C3 122.38(14). (b) **3**; Selected bond lengths (Å) and bond angles (deg): Si1-C1 1.8814(14); C2-C3 1.3988(18); C3-C4 1.4199(18); Si1-C1-C2 121.98(10) C1-C2-C3 122.41(12).

The absorption spectra of hexane solutions of the silylpyrenes were investigated in the range 290−400 nm (Fig. 2). In this spectral region two lowest transitions are observed. An intense absorption band around 340 nm with vibronic structures

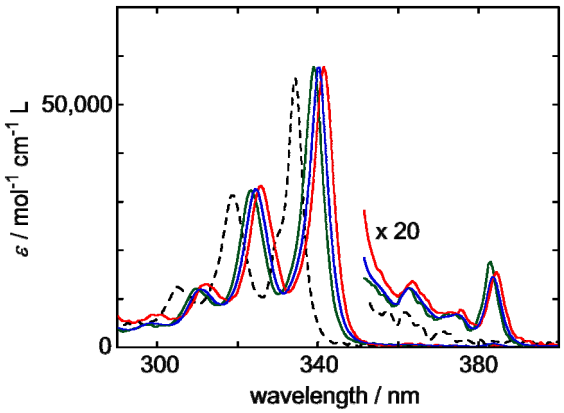

Fig. 2. Absorption spectra of 1,4-bissilylpyrenes in *n*-hexane (290−400 nm) [parent pyrene (broken black line), **3** (solid green line), **1** (solid red line), and **1i** (solid blue line)].

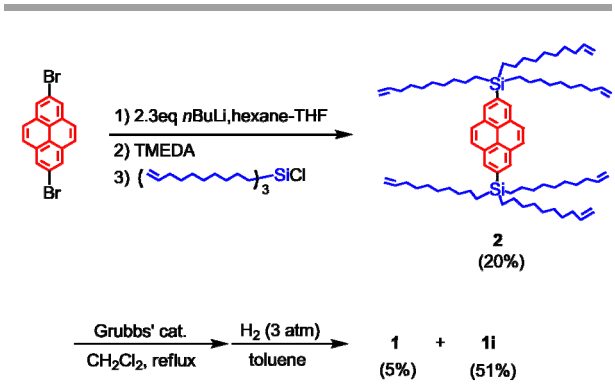

Scheme 1. Synthesis of Molecular Gyrotop **1**.

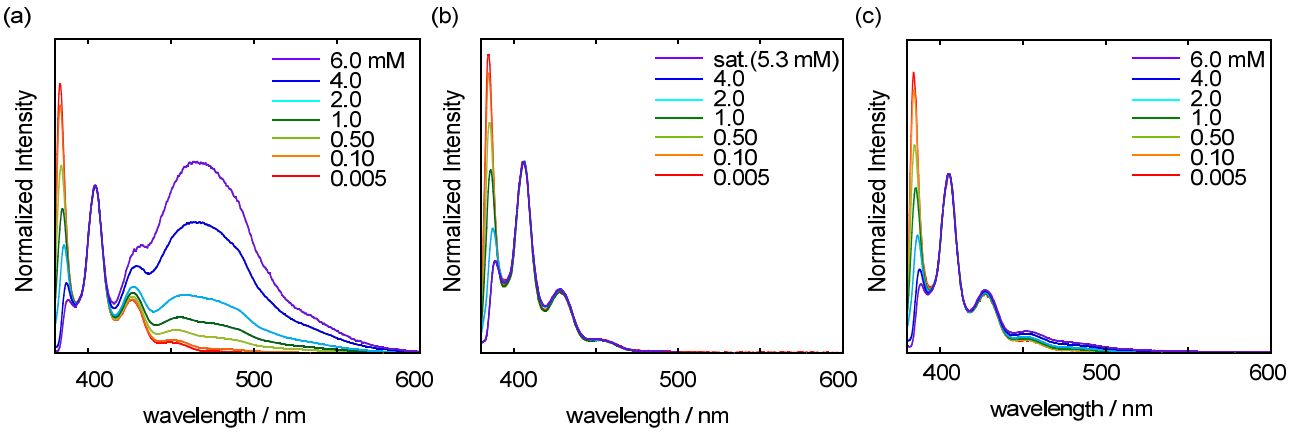

Fig. 3. Fluorescence spectra of 1,4-bissilylpyrenes in *n*-hexane: (a) **3**, (b) **1**, (c) **1i**. The intensities were normalized at the second vibronic band maxima of unassociated fluorescence.

Table 1. Fluorescence Parameters of Bissilylpyrenes in n-Hexane

Compound	Φ [a]	τ_0 [b] / ns	Fluorescence Quenching by Nitrobenzene: Parameters for Stern-Volmer Plot					
			Method	K_D [e] / M^{-1}	y-intercept	R^2 [f]	k_q [g] / $M^{-1}s^{-1}$	K_D_τ / K_D_F
Pyrene	0.52[10a]	452	F_0/F [c]	1.32×10^4	1.03	0.994	2.91×10^{10}	1.02
			τ_0/τ [d]	1.34×10^4	1.02	0.997	2.96×10^{10}	
3	0.68	213	F_0/F [c]	4.60×10^3	0.969	0.998	2.13×10^{10}	0.976
			τ_0/τ [d]	4.49×10^3	0.994	0.987	2.14×10^{10}	
1	0.63	216	F_0/F [c]	2.77×10^3	1.02	0.997	1.21×10^{10}	1.01
			τ_0/τ [d]	2.81×10^3	1.02	0.998	1.25×10^{10}	
1i	0.68	212	F_0/F [c]	3.34×10^3	0.988	0.996	1.47×10^{10}	1.02
			τ_0/τ [d]	3.40×10^3	1.00	0.999	1.46×10^{10}	

[a] The quantum yields were determined by comparing the fluorescence intensity of pyrene in hexane (Φ = 0.52 Ref 10a)) under irradiation with 303 nm light. [b] The lifetimes were measured in 1.0 μM solution under the irradiation of 340 nm light with a time-correlated single-photon counting apparatus. [c] Fluorescence intensity ratio [intensity at 385 nm (excited at 340 nm)]. [d] The lifetimes were measured at 385 nm under the irradiation of 340 nm light. [e] Estimated from the slope of the plot. [f] Correlation coefficient. [g] Calculated by the following relation: $k_q = K_D/\tau_0$.

can be assigned to Platt's ^1L_a band and a weak band at 380 nm can be assigned to the ^1L_b band.[8] The red-shift of the bands in the absorption spectra of silylpyrenes has been reported to be due to σ*-π* conjugation.[1a,9] The absorption bands of the present silylpyrenes, i.e., caged pyrene **1,** the non-caged isomer **1i** and **3**, were confirmed to be slightly red-shifted compared with those of the parent pyrene.

Fluorescence spectra in various concentrations

Fig. 3 shows the fluorescence spectra of **1**, **1i,** and **3** in various concentrations of hexane; the spectra were normalized at the second vibronic-band maxima of unassociated fluorescence. Notably, the first vibronic band in all the spectra could be assigned to the 0–0 transition; its intensity decreased with increasing concentration because of self-absorption. Pyrene and its derivatives are known to show excimer fluorescence under high solution concentration. Indeed, the fluorescence spectra of **3** in 6 mM hexane solution exhibit broad excimer fluorescence (470 nm) as well as an unassociated fluorescence (385 nm) with vibronic structure.

The intensity of the excimer fluorescence increased with increasing concentration. The fluorescence spectrum of the 6 mM hexane solution of the non-caged isomer **1i** also showed excimer fluorescence. On the other hand, the spectrum of **1** under the saturated conditions of 5.3 mM hexane, which is estimated from absorbance, showed only local emission with vibronic structure and no excimer fluorescence was observed. These results indicate that the cage structure of **1** inhibits the formation of the excimer due to protective steric effects. The other fluorescence properties of **1** were similar to those of **3** and **1i**. The unassociated fluorescence maxima of **1**, **3** and **1i** were 385, 388, and 388 nm, respectively. The quantum yields and lifetimes (1 μM) of the unassociated fluorescence were 0.63, 216 ns for **1**; 0.68, 213 ns for **3;** and 0.68, 212 ns for **1i**.

Fluorescence quenching experiments

The fluorescence intensity is known to be reduced in the presence of quenchers, known as fluorescence quenching.[11] Usually, the efficiency of fluorescence quenching is analyzed by the Stern-Volmer equation (eq. 1).[11] In this equation, F_0 and F are the fluorescence intensities in the absence and the

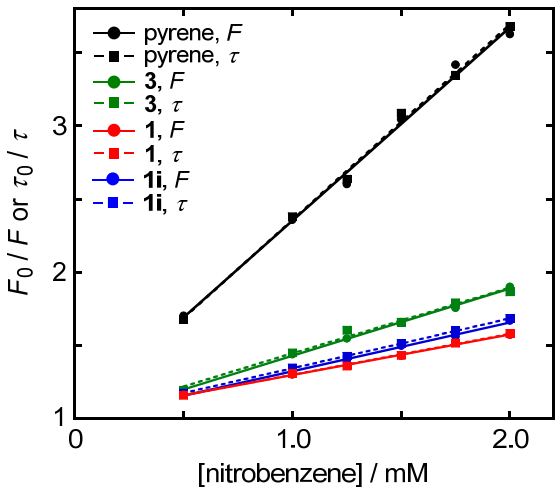

Fig 4. Stern-Volmer plots for quenching of the unassociated fluorescence of the pyrene derivatives by nitrobenzene. Intensity plots are indicated by solid lines with solid circles and lifetime plots are indicated by broken lines with solid squares. [Pyrene (black, excitation (ex) at 334 nm, emission (em) at 383 nm), **3** (green, ex 339 nm, em 384 nm), **1** (red, ex 341 nm, em 385 nm), and **1i** (blue, ex 340 nm, em 385 nm)].

presence of the quencher, respectively, and $[Q]$ is the concentration of the quencher. A plot of F_0/F *versus* $[Q]$ affords a slope of K_D and an intercept of 1. K_D is called the Stern-Volmer quenching constant and is given by $K_D = k_q \tau_0$, where k_q and τ_0 are the bimolecular quenching constant and the fluorescence lifetime in the absence of the quencher, respectively. The k_q reflects the efficiency of fluorescence quenching. The value of k_q is almost 1.0×10^{10} M^{-1} s^{-1}, indicating that the quenching is diffusion-controlled. If k_q is smaller than the diffusion-controlled value, steric shielding of the fluorophore or low quenching efficiency should be considered.

$$\frac{F_0}{F} = K_D[Q] + 1 \qquad (1)$$

The fluorescence of pyrene, silylpyrene **3**, caged pyrene **1**, and the non-caged isomer **1i** were investigated in the presence of nitrobenzene as a quencher. Fig. 4 shows the Stern-Volmer plots (F_0/F versus $[Q]$) for the fluorescence quenching experiments. The linearity of the plots indicates the single class of the fluorescence quenching. Plots of τ_0/τ versus $[Q]$ are also shown in Fig. 4, in which lifetimes were determined by single-photon-counting methods. If fluorescence quenching occurs by intermolecular collision between the fluorophore and the quencher, i.e., "dynamic quenching", the quencher concentration dependence of the ratio of intensities F_0/F is identical to the ratio of lifetimes τ_0/τ .[11] The present data showed that the slopes of both the intensity Stern-Volmer plots (K_D_F) and the lifetime Stern-Volmer plots (K_D_τ) were completely identical ($K_D\_\tau/K_D\_F \sim 1$), indicating that quenching is caused by collision. The Stern-Volmer constants, K_Ds, estimated by the slopes of the plots are summarized in Table 1. The bimolecular quenching constants k_q, calculated by $k_q = K_D/\tau_0$, are also summarized in Table 1. Although the values of k_q were close to the diffusion-controlled limits (ca. 10^{10}), k_q of **1** is slightly smaller than that of **1i**. Since the molecular size of **1** is the same or slightly smaller than that of **1i**, the small k_q of **1** (1.2×10^{10} M^{-1} s^{-1}) compared with **1i** (1.5×10^{10} M^{-1} s^{-1}) indicates that the cage sterically shields the pyrene fluorophore.

Conclusions

In summary, a cage-like cyclophane of pyrene **1** was first designed and synthesized. The fluorescence properties of the caged pyrene **1** were investigated and compared with those of the non-caged pyrenes (**1i** or **3**). Although pyrene shows excimer fluorescence in highly concentrated solutions, the caged pyrene **1** shows no excimer fluorescence, even in saturated solution, indicating that the steric shielding by the cage prevents the formation of the excimer. The efficiency of the fluorescence quenching in **1** was also investigated. The lower quenching efficiency of **1** as a result of the cage was revealed by analysis of the bimolecular quenching constants k_q. The studies of the cage effects of **1** can be investigated theoretically, although it is necessary to improve the solubility of compound for practical applications as biomerkers.

Experimental

General methods

All reactions were conducted under an argon atmosphere. Chemical shifts of the ^{1}H and ^{13}C NMR spectra were calibrated using the residual solvent resonance except for ^{29}Si NMR. ^{29}Si chemical shifts were referenced to external tetramethylsilane. NMR signals were assigned by applying 1D and 2D NMR techniques (^{1}H, ^{13}C, DEPT, COSY, and HSQC). Commercially available reagents were used without further purification.

Synthesis

Synthesis of 2,7-Bis(tri-9-decenylsilyl)pyrene (2). 2,7-dibromopyrene (300 mg, 0.833 mmol) and dry tetrahydrofuran (THF) (9 mL) were placed in a Schlenk flask (200 mL). *n*-BuLi solution (1.6 M in hexane, 2.1 mL, 1.0 equiv.) was added dropwise to the flask for 15 min at −78°C. The reaction mixture was warmed to room temperature for 1 h. After addition of tetramenylethylenediamine (TMEDA, 193 mg, 1.66 mmol), tri(9-decenyl)chlorosilane[4a] (981 mg, 1.94 mmol) was added at rt. The reaction mixture was stirred for 12 h at rt. The mixture was hydrolyzed with dilute HCl (aq) solution and extracted with hexane. The organic layer was washed with saturated $NaHCO_3$ (aq) solution and dried over anhydrous Na_2SO_4. Silica gel column chromatography of the concentrated residue afforded crude **2** as a colorless oil (618 mg). Purification of crude **2** was treated with GPC (chloroform), and the solvents were evaporated. Pure compound **2** (180 mg, 0.165 mmol, 19.8% yield) was obtained as a colorless oil. **2**; a colorless oil; ^{1}H NMR (500 MHz, $CDCl_3$) δ 0.974 (m, 12H), 1.20-1.42 (m,

72H), 2.00 (q, J = 5.7 Hz, 12H), 4.90 (d, J = 8.2 Hz, 6H), 4.96 (d, J = 13.4 Hz, 8H), 5.76 (ddt , J = 13.4 Hz, 8.2 Hz, 5.7 6H), 8.05 (s, 4H) , 8.24 (s, 4H); ^{13}C NMR (126 MHz, $CDCl_3$) δ 12.7, 23.9, 28.9, 29.1, 29.2, 29.4, 33.7, 33.8, 114.1, 124.9, 127.3, 130.4, 130.6, 135.9, 139.3; ^{29}Si NMR (99 MHz, $CDCl_3$) δ −1.04; HRMS (ESI positive) *m/z* calcd for $C_{76}H_{122}Si_2$+Na^+: 1113.89773 found: 113.89797.

Synthesis of pyrene-bridged molecular gyrotop (1) and its isomer (1i). To a solution of first-generation Grubbs' catalyst (0.05 g, 0.06 mmol) in dichloromethane (500 mL), 2,7-Bis(tri-9-decenylsilyl)pyrene (**2**) (553 mg, 506 mmol) in dichloromethane (200 mL) was added dropwise while stirring over 10 h, and the mixture was further stirred for 14 h. The volatile materials were removed *in vacuo*, and the metal catalyst was removed from the toluene-soluble fraction by flash column chromatography (silica gel, benzene). Hydrogen gas (3 atm) was then introduced in an autoclave to a solution of toluene (5 mL) and the reaction mixture in the presence of 10% Pd/C (0.03 g), and the mixture was allowed to stand for 72 h at 60°C. After the excess H_2 gas was released, the mixture was filtered to remove the Pd/C. The volatile materials were removed *in vacuo*. The fractions containing **1** and **1i** were collected separately by GPC (chloroform), and the solvents were evaporated. Pure compound **1** (28 mg, 0.028 mmol, 5.5% yield) was obtained as colorless crystals by recrystallization from THF/methanol (4:1). Pure compound **1i** (261 mg, 0.257 mmol, 51% yield) was obtained without further purification. **1**; colorless crystals, mp 280-282°C, ^{1}H NMR (500 MHz, $CDCl_3$) δ 0.94 (m, 12H), 1.10-1.45 (m, 96H), 8.04 (s, 4H), 8.29 (s, 4H); ^{13}C NMR (126 MHz, $CDCl_3$) δ 13.3, 23.3, 28.1, 28.6, 29.5, 29.6, 30.0, 30.0, 32.7, 124.9, 127.3, 130.5, 131.0, 135.5; ^{29}Si NMR (99 MHz, $CDCl_3$) δ −0.87; HRMS (ESI positive) *m/z* calcd for $C_{70}H_{116}Si_2$+Na^+: 1035.85078 found: 1035.85095. **1i**; a colorless oil, ^{1}H NMR (500 MHz, $CDCl_3$) δ 0.8-1.5 (m, 108H), 8.07 (s, 4H), 8.27 (s, 4H); ^{13}C NMR (126 MHz, $CDCl_3$) δ 12.1, 13.4, 23.4, 23.5, 27.4, 27.7, 28.1, 28.2, 28.5, 28.6, 28.7, 28.7, 29.1, 29.4, 29.6, 29.7, 33.2, 33.3, 124.9, 127.4, 130.4, 130.7, 136.0; ^{29}Si NMR (99 MHz, CDCl3) δ −0.53; HRMS (ESI positive) *m/z* calcd for $C_{70}H_{116}Si_2$+Na^+: 1035.85078 found: 1035.85091.

Synthesis of 2,7-Bis(trimethylsilyl)pyrene (3). 2,7-dibromopyrene (1.00 g, 2.78 mmol) and dry tetrahydrofuran (THF) (30 mL) were placed in a Schlenk flask (200 mL). *n*-BuLi solution (1.6 M in hexane, 7.0 mL, 4.0 equiv.) was added dropwise to the flask at −78°C, and stirred for an additional 2 h. After the reaction mixture was warmed to room temperature, trimethylchlorosilane (692 mg, 6.92 mmol) was added and stirred for 12 h at rt. The mixture was hydrolyzed with dilute HCl (aq) solution and extracted with hexane. The organic layer was washed with saturated $NaHCO_3$ (aq) solution and dried over anhydrous Na_2SO_4. Recrystallization from dichloromethane solution of the crude product afforded **3** as colorless crystals (535 mg, 1.64 mmol, 55.6% yield). **3**; colorless crystals; mp 204-206 °C; ^{1}H NMR (500 MHz, $CDCl_3$) δ 0.51 (s, J = 9 Hz, 12H, Si-CH_2-), 8.09(s, 4H), 8.34(s, 4H); ^{13}C NMR (126 MHz, $CDCl_3$) δ −0.7, 125.0, 127.5, 129.9, 130.5, 138.2; ^{29}Si NMR (99 MHz, $CDCl_3$) δ −3.05; HRMS (ESI positive) *m/z* calcd for $C_{22}H_{26}Si_2$+Na^+: 369.14652 found: 369.14651.

X-ray crystallography

The diffraction data of silylpyrenes **1** and **3** were collected using graphite-monochromatized MoK_α radiation (λ = 0.71069 Å). Crystal data for **1** at 100 K, triclinic, P-1, a = 12.173(3) Å, b = 17.375(4) Å, c = 18.275(4) Å, α = 61.920(3)°, β = 71.547(3)°, γ = 87.263(3)°, V = 3211.3(14) Å^3, $R1$ = 0.0575 ($I > 2\sigma I$), $wR2$ = 0.1553 (all data). Crystal data for **3** at 100 K, monoclinic, $P2_1/c$, a = 6.3540(12) Å, b = 16.626(3) Å, c = 9.3688(17) Å, α = 90°, β = 100.456(2)°, γ = 90°, V = 973.3(3) Å^3, $R1$ = 0.0331 ($I > 2\sigma I$), $wR2$ = 0.0905 (all data). Crystallographic data were deposited in the Cambridge Crystallographic Database Centre (CCDC-1415849 for **1**, CCDC-1415850 for **3**).

Fluorescence study

The fluorescence spectra were measured using a JASCO FP-8300 spectrometer. The fluorescence lifetimes were measured using a HAMAMATSU Quantaurus-tau fluorescence lifetime spectrometer. The samples with various concentrations for fluorescence spectra (Fig. 3) were degassed by argon bubbling before the measurements. Quantum yield and lifetime (Table 1) measurements and fluorescence quenching experiments (Table 1 and Fig. 4) were carried out with samples thoroughly degassed by several freeze–pump–thaw sequences.

In the fluorescence intensity quenching experiments (the intensity Stern–Volmer plots in Fig. 4), with nitrobenzene as the quencher, nitrobenzene absorbs the excitation light (ε = 117 mol^{-1} cm^{-1} L at 340 nm in hexane). Therefore, the intensities of the observed fluorescence in the presence of nitrobenzene were calibrated by the ideal transmittance of the excitation light derived from the absorbance at each concentration of nitrobenzene.

Conflict of interest

The authors declare no competing financial interests.

Acknowledgements

This work was supported by a JSPS Grant-in-Aid for Scientific Research on Innovation Areas "stimuli-responsive chemical species" (WS, no. 15H00955) and Scientific Research (B) (WS and KY, no. 25288042).

Notes and references

1 For recent reviews on the fluorescence of pyrenes, see: (a) K. Shinozuka and T. Takeuchi, In *Pyrene*, P. Ruzicka and T. Kral, Eds.; Nova Science Publishers, Inc: Hauppauge, N. Y., 2013, pp 167-187; (b) J. Duhamel, *Langmuir*, 2014, **30**, 2307; (c) Y. Niko, Y. Hiroshige, S. Kawauchi and G. Konishi, *Tetrahedron*, 2012, **68**, 6177; (d) J. Duhamel, *Polymers (Basel, Switzerland)*, 2012, **4**, 211; (e) E. Manandhar and K. J. Wallace, *Inorg. Chim. Acta*, 2012, **381**, 15.

2 (a) P. Commins and M. A. Garcia-Garibay, *J. Org. Chem*., 2014, **79**, 1611; (b) B. Rodríguez-Molina, S. Pérez-Estrada and M. A. Garcia-Garibay, *J. Am. Chem. Soc.*, 2013, **135**, 10388; (c) C. S. Vogelsberg and M. A. Garcia-Garibay, *Chem. Soc. Rev.*, 2012, **41**, 1892; (d) D. Czajkowska-Szczykowska, B. Rodríguez-Molina, N. E. Magaña-Vergara, R. Santillan, J. W. Morzycki and M. A. Garcia-Garibay, *J. Org. Chem.*, 2012, **77**, 9970; (e) P. Commins, J. E. Nuñez and M. A. Garcia-Garibay, *J. Org. Chem.*, 2011, **76**, 8355; (f) J. E. Nuñez, A. Natarajan, S. I. Khan and M. A. Garcia-Garibay, *Org. Lett.*, 2007, **9**, 3559; (g) M. A. Garcia-Garibay, *Proc. Nat. Acad. Sci. USA*, 2005, **102**, 10771.

3 (a) A. J. Nawara-Hultzsch, M. Stollenz, M. Barbasiewicz, S. Szafert, T. Lis, F. Hampel, N. Bhuvanesh and J. A. Gladysz, *Chem. Eur. J.*, 2014, **20**, 4617; (b) P. D. Zeits, G. P. Rachiero, F. Hampel, J. H. Reibenspies and J. A. Gladysz, *Organometallics*, 2012, **31**, 2854; (c) K. Skopek and J. A. Gladysz, *J. Organomet. Chem.*, 2008, **693**, 857; (d) K. Skopek, M. Barbasiewicz, F. Hampel and J. A. Gladysz, *Inorg. Chem.*, 2008, **47**, 3474; (e) J. Han, C. Deng, R. Fang, D. Zhao, L. Wang and J. A. Gladysz, *Organometallics*, 2010, **29**, 3231; (f) G. D. Hess, F. Hampel and J. A. Gladysz, *Organometallics*, 2007, **26**, 5129; (g) L. Wang, T. Shima, F. Hampel and J. A. Gladysz, *Chem. Commun.*, 2006, 4075; (h) L. Wang, F. Hampel and J. A. Gladysz, *Angew. Chem. Int. Ed.*, 2006, **45**, 4372; (i) A. J. Nawara, T. Shima, F. Hampel and J. A. Gladysz, *J. Am. Chem. Soc.*, 2006, **128**, 4962; (j) T. Shima, F. Hampel and J. A. Gladysz, *Angew. Chem. Int. Ed.*, 2004, **43**, 5537.

4 (a) W. Setaka, K. Inoue, S. Higa, S. Yoshigai, H. Kono and K. Yamaguchi, *J. Org. Chem.*, 2014, **79**, 8288; (b) W. Setaka, S. Higa and K. Yamaguchi, *Org. Biomol. Chem.*, 2014, **12**, 3354; (c) Y. Inagaki, K. Yamaguchi and W. Setaka, *RSC Adv.*, 2014, **4**, 58624; (d) W. Setaka and K. Yamaguchi, *J. Am. Chem. Soc.*, 2013, **135**, 14560; (e) W. Setaka, A. Koyama and K. Yamaguchi, *Org. Lett.*, 2013, **15**, 5092; (f) W. Setaka and K. Yamaguchi, *Proc. Natl. Acad. Sci. U.S.A.*, 2012, **109**, 9271; (g) W. Setaka and K. Yamaguchi, *J. Am. Chem. Soc.*, 2012, **134**, 12458.

5 (a) W. Setaka, S. Ohmizu and M. Kira, *Chem. Commun.*, 2014, **50**, 1098; (b) A. B. Marahatta, M. Kanno, K. Hoki, W. Setaka, S. Irle and H. Kono, *J. Phys. Chem. C*, 2012, **116**, 24845; (c) W. Setaka, S. Ohmizu and M. Kira, *Chem. Lett.*, 2010, **39**, 468; (d) W. Setaka, S. Ohmizu, C. Kabuto and M. Kira, *Chem. Lett.*, 2007, **36**, 1076.

6 For recent reviews on cyclophane chemistry, see: (a) V. I. Rozenberg, E. V. Sergeeva and H. Hopf, In *Modern Cyclophane Chemistry*; R. Gleiter and H. Hopf, Eds.; Wiley-VCH: Weinheim, 2004; (b) F. Vögtle, *Cyclophane Chemistry, Synthesis, Structure and Reactions*; Wiley: Chichester, 1993.

7 (a) T. Yorozu, M. Hoshino and M. Imamura, *J. Phys. Chem*., 1982, **86**, 4426; (b) Y. Yamauchi, M. Yoshizawa, M. Akita and M. Fujita, *Proc. Natl. Acad. Sci. U.S.A.*, 2009, **106**, 10435; (b) N. Hafezi, J. M. Holcroft, K. J. Hartlieb, E. J. Dale, N. A. Vermeulen, C. L. Stern, A. A. Sarjeant and J. Fraser Stoddart, *Angew. Chem. Int. Ed.*, 2015, **54**, 456; (b) J. H. Jordan and B. C. Gibb, *Chem. Soc. Rev.*, 2015, **44**, 547.

8 (a) A. Bree and V. V. B. Vilkos, *J. Chem. Phys.*, 1964, **40**, 3125; (b) N. S. Ham and K. Ruedenberg, *J. Chem. Phys*., 1956, **25**, 13.

9 (a) S. Kondo, Y. Bie and M. Yamamura, *Org. Lett*., 2013, **15**, 520; (b) Y. Niko, S. Kawauchi, S. Otsu, K. Tokumaru and G. Konishi, *J. Org. Chem.*, 2013, **78**, 3196; (c) K. Imai, T. Sasaki, J. Abe, A. Kimoto, Y. Tamai and N. Nemoto, *Polymer J.*, 2009, **41**, 584; (d) D. Declercq, P. Delbeke, F. C. Schryver, L. Meervelt and R. D. Miller, *J. Am. Chem. Soc.*, 1993, **115**, 5702.

10 (a) D. S. Karpovich and G. J. Blanchard, *J. Phys. Chem*., 1995, **99**, 3951; (b) W. D. Dawson and M. W. Windsor, *J. Phys. Chem.*, 1968, **72**, 3251; (c) H. Kashida, K. Sekiguchi, N. Higashiyama, T. Kato and H. Asanuma, *Org. Biomol. Chem*., 2011, **9**, 8313.

11 J. R. Lakowicz, In *Principles of Fluorescence Spectroscopy, 3rd Ed.*; Springer: New York, 2006, chapter 8.